Learning Suction Cup Dynamics from Motion Capture: Accurate Prediction of an Object's Vertical Motion during Release

Menno L S Lubbers, Job van Voorst, Maarten Johannes Jongeneel, Alessandro Saccon

 DOI: https://doi.org/10.1109/IROS47612.2022.9982211

Learning Suction Cup Dynamics from Motion Capture: Accurate Prediction of an Object's Vertical Motion during Release

Menno Lubbers, Job van Voorst, Maarten Jongeneel*, and Alessandro Saccon

***Abstract*— Suction grippers are the most common pick-and-place end effectors used in industry. However, there is little literature on creating and validating models to predict their force interaction with objects in dynamic conditions. In this paper, we study the interaction dynamics of an active vacuum suction gripper during the vertical release of an object. Object and suction cup motions are recorded using a motion capture system. As the object's mass is known and can be changed for each experiment, a study of the object's motion can lead to an estimate of the interaction force generated by the suction gripper. We show that, by learning this interaction force, it is possible to accurately predict the object's vertical motion as a function of time. This result is the first step toward 3D motion prediction when releasing an object from a suction gripper.**

I. Introduction

Due to the ability to deal with objects of various shapes, materials, and sizes, suction cups are common pick-and-place end effectors used in industry. In recent years, due to labor scarcity, ergonomic considerations, and booming of e-commerce, the development of autonomous pick-and-place solutions for (de)palletizing, order fulfillment/packaging, and bin-to-belt/bin-to-bin applications is steadily growing. See, e.g., [1] for a commercially available solution in warehousing. The robotics literature dealing with perception and control of robots employing suction cups is correspondingly growing, e.g., providing frameworks for order packing [2] or selection of robust vacuum suction grasp targets starting from point clouds [3], employing quasi-static spring modeling assumptions. Suction cups have the potential to be used for dexterous manipulation [4], aside from standard pick-and-place, including the possibility to execute pushing, dragging [2] or toppling motions [5]. Due to a partial vacuum, they have the extra feature of allowing for bilateral contact: to pull and not just push. Robotic tossing using suction cups is also receiving increased attention. For suction cups, separating recyclables into bins by tossing instead of placing is becoming a common solution in automated urban waste sorting facilities, using the combination of suctions grippers and delta robots as, e.g., in [6], [7] or employing collaborative robots [8]. Scientific literature about robotic tossing with suction cups is starting to appear. In [9], it is reported that pick-and-toss reduces the time of processing recyclable items by 15,3% in comparison to traditional pick-and-place.

This work was partially supported by the Research Project I.AM. through the European Union H2020 program under GA 871899.

M. Lubbers, J. van Voorst, M. J. Jongeneel (*Corresponding author), and A. Saccon are with Faculty of Mechanical Engineering, Eindhoven University of Technology (TU/e), The Netherlands {m.l.s.lubbers, j.v.voorst}@student.tue.nl, {m.j.jongeneel, a.saccon}@tue.nl

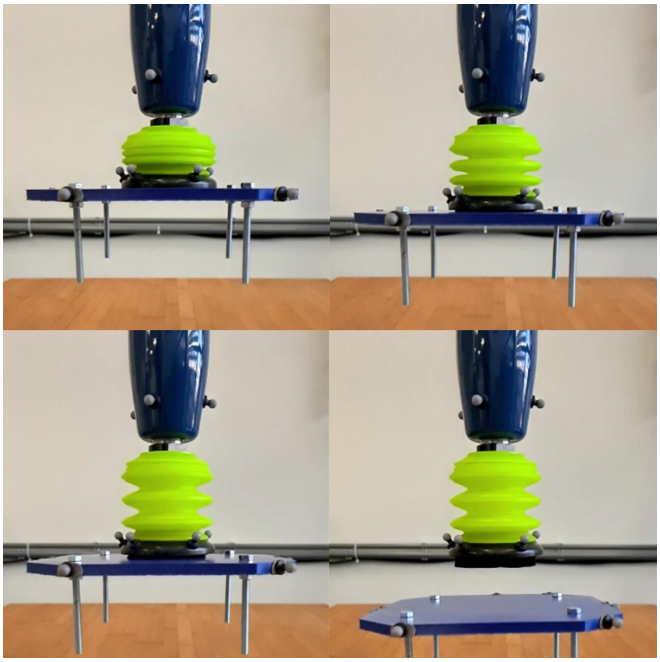

Fig. 1: Snapshots of a slow motion recorded video during a typical vertical dropping experiment. The object is a plastic plate, that provides a sealant surface and four metal rods that are used to attach additional weights. The whole sequence takes less than 150 ms.

Contribution. In this paper, we specifically look at the release dynamics of an active vacuum suction cup. The suction cup is provided with an active vacuum created by a Venturi ejector. During the release, the ejector valve is closed and compressed air is injected into the suction cup via a separate channel to speed up the release. The motion of the suction cup mounting point, suction cup lip, and the object is measured using a motion capture system (360 Hz sampling rate, with sub-millimeter accuracy). We show that, during the release, it is possible to accurately predict the motion of the object over time, just knowing its mass, position, and velocity at the moment of release. In particular, the obtained force model is capable of reproducing, both qualitatively and quantitatively, the quite rich acceleration and velocity profile of the released object. To the best of the authors' knowledge, it is the first time that such a detailed prediction is attempted and validated for an active suction cup gripper during release.

Related literature. Despite the existing efforts, there is little literature regarding creating model-based or data-driven models to predict object-suction-cup interaction in dynamic conditions. The majority of existing studies employ a quasi-static assumption in modeling the suction cup dynamics.

For example, in [4], the authors employ a locally linear force-deformation model that is fitted online starting from a deformation-reaction force dataset, previously obtained using a force-torque sensor. Given a measured wrench, their approach allows computing an estimate of the suction cup deformation, which is then used for manipulation purposes. In [10], a quite detailed physics-based model of a suction cup is provided. It is obtained by discretization of a CAD drawing into a FEM mesh. It includes force-contact complementary conditions to include contact and force constraints and determines air tightness to impose the pressure within the suction cup cavity. The model is that of a passive vacuum suction cup (i.e., no pump or vacuum ejector is considered), and without bellows. For the same type of passive vacuum suction cup, [11] provides a detailed study of gas and water leakage, which is of interest for obtaining estimates of the suction cup's failure time. In [12], the authors study the problem of fast pick-and-place systems with suction cups, where they only consider the maximum forces that prevent suction cup detachment while moving an object. More recently, [13] investigates fast vertical picking, employing a linear visco-elastic model to model the suction cup force during contact. Active-vacuum suction cups in dynamic holding conditions are also studied in [14] with the goal of improving energy efficiency in handling processes. The paper considers the 1D dynamic deformation behavior of vacuum grippers in interaction with specific gripper-object combinations (metal objects with concave/convex and flat/curved surfaces), imposing a predetermined force-deformation stiffness model whose parameters are then learned from quasi-static experiments. A parametric position-dependent nonlinear damping model is then tuned by means of pull-off experiments conducted at different velocities.

Paper structure. Besides this introduction, this paper is structured as follows. The description of the experimental setup is provided in Section II. Section III provides the mathematical formulation of the problem, together with a fundamental assumption that allows to arrive at a simplified force model. The simplified formulation is used in Section IV to learn a model from data and to validate the approach. The conclusion and recommendations for future work are given in Section V.

II. Experimental setup

As illustrated in Figure 2, the experimental setup consists of a 6-axis UR10 collaborative robot arm by Universal Robots equipped with an industrial vacuum gripper produced by the company Smart Robotics. The gripper is provided with a piGRIP suction cup, produced by Piab. As shown in Figure 3a, the suction cup consists of four main parts: the mounting point, the bellows, the suction cup lip, and the foam. The mounting connects the suction cup to the vacuum gripper. The suction cup has three bellows, which allow it to adapt in the cup's longitudinal direction when a vacuum is created inside the suction cup cavity to grab/hold an object.

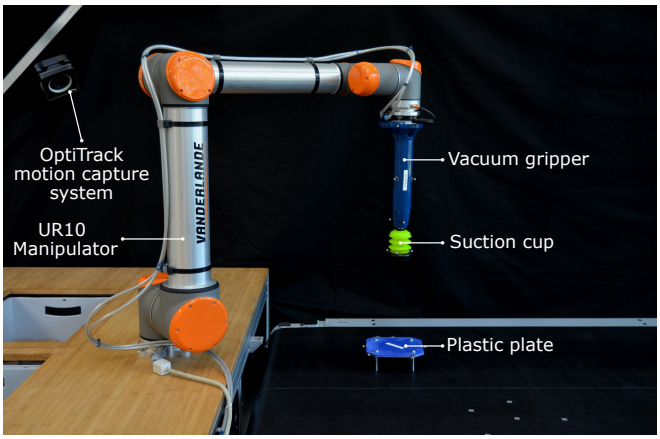

Fig. 2: Experimental setup. A motion capture system is employed to record the motion of the vacuum gripper, suction cup, and test object during vertical release. To replicate intended mounting conditions, the suction gripper is mounted on a collaborative robot.

The suction cup ends with a plastic plate with soft foam to ensure extra sealing and adaptability to objects of various surface shapes.

The vacuum gripper has two functional modalities: it can create an under-pressure or over-pressure. A vacuum is created by a Venturi ejector which is fed by a compressed air tank. Over-pressure is created by injecting the compressed air from the tank into the suction cup, bypassing the ejector, to speed up object release. We refer to this modality as *blow-off*. A 3D printed plastic plate is used as a release object, ensuring a sealant surface for the suction gripper. Four metal rods attached to the plastic plate allow to fasten different weights and change the total mass. An OptiTrack motion capture system consisting of 6 infrared cameras (four Prime 17W and two Prime x22 cameras) surrounds the robotic setup. This system tracks the vacuum gripper, suction cup lip, and plastic plate, each containing six passive reflective markers. In Motive, the software package of the motion capture system, rigid bodies are defined using these sets of markers that allows us to track the vacuum gripper, suction cup lip, and the plastic plate by means of the distances a, h_{sc}, and h, respectively, as also depicted in Figure 3.

III. Problem and mathematical formulation

Problem formulation. *Devise and validate an approach to learn a force model for an active vacuum suction gripper capable of predicting the motion for a series of objects of known mass, as a function of the initial position and velocity of the object at the release moment. The data available for this task are the time series of the position of the mounting point, suction cup lip, and objects during the release.*

For the tossing object employed in this study, we assume that the the aerodynamic drag force is negligible (free falling), and we will confirm this in Section IV. From this assumption follows that the vertical object motion satisfies

$$m\ddot{h} = -mg - f_{\text{scup}\to\text{obj}} + f_{\text{air}\to\text{obj}}, \tag{1}$$

where m denotes the object mass (assumed to be directly centered under the suction cup), h denotes the object height

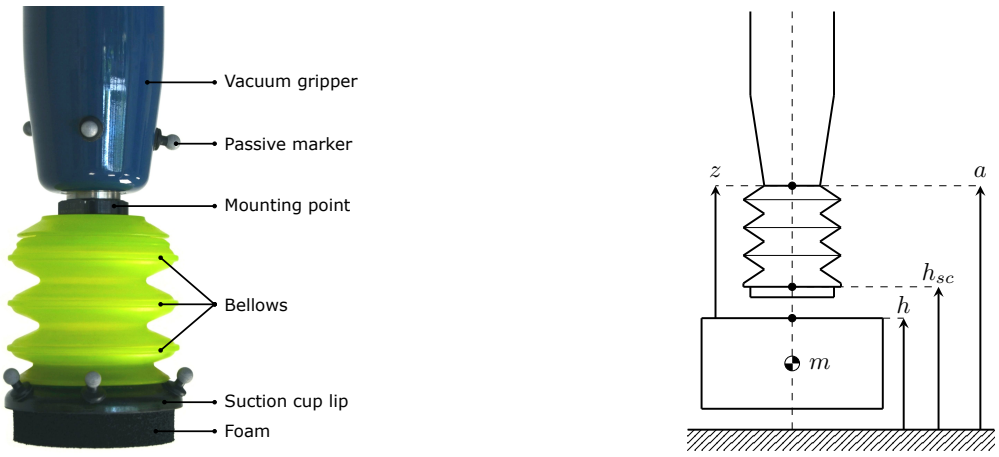

(a) (b)

Fig. 3: Employed suction gripper. (a) Close-up of the vacuum gripper with bellows suction cup, showing the passive motion-capture markers; (b) Definition of parameters; height of the suction cup mounting point a; height of the suction cup lip h_{sc}; height of the top of the object h; and relative distance between the top of the package and the suction cup mounting point z. Note that $a = h + z$.

with respect to the fixed world, $g = 9.81m/s^2$ is the gravitational acceleration, $f_{\text{scup}\to\text{obj}}$ is the mechanical force applied by the suction cup lip on the object, $f_{\text{air}\to\text{obj}}$ is the force induced by the suction and blow-off of the suction cup applied to the object. Note that when the suction cup is no longer in physical contact with the object $f_{\text{scup}\to\text{obj}} = 0$. From basic physical considerations, the reaction force $f_{\text{scup}\to\text{obj}}$ is also applied in the opposite direction to the suction cup. The suction cup is a continuum deformable model, but taking a lumped parameter model as an approximation and denoting by m_{sc} its equivalent moving mass, the simplified lumped dynamics of the suction cup can be written as

$$m_{sc}\ddot{h}_{sc} = -m_{sc}g + f_{\text{stiff-damp}} + f_{\text{scup}\to\text{obj}} + f_{\text{air}\to\text{scup}} \quad (2)$$

where h_{sc} denotes the height of the suction cup lip as in Figure 3b, $f_{\text{stiff-damp}}$ the stiffness-and-damping force depending on h_{sc} and $\dot{h}_{sc}$, $f_{\text{scup}\to\text{obj}}$ the mechanical reaction force of the object applied to the suction cup lip, and $f_{\text{air}\to\text{scup}}$ fluid dynamics forces acting along the suction cup axis. At the beginning of the release phase, the object is still attached to the suction cup lip. This means we can state that $h = h_{\text{sc}}$, and thus summing up (1) and (2) leads to

$$m_{\text{tot}}\ddot{h} = -m_{tot}g + f_{\text{stiff-damp}} + f_{\text{air}\to\text{scup}} + f_{\text{air}\to\text{obj}}, \quad (3)$$

with $m_{\text{tot}} := m + m_{\text{sc}}$. In an attempt to find a dynamical model that describes the motion of the object during the entire release phase, we observe that it is sufficient to model the total force exerted by the suction cup and the air, so $f_{\text{scup+air}\to\text{obj}} := f_{\text{air}\to\text{obj}} - f_{\text{scup}\to\text{obj}}$. From an abstract perspective, we see that

$$f_{\text{scup+air}\to\text{obj}} = f_{\text{scup+air}\to\text{obj}}(\text{state}_{\text{obj}}, \text{state}_{\text{scup}}, \text{state}_{\text{air}}, m), \quad (4)$$

where $\text{state}_{\text{obj}}$ represents the relative position and velocity of the object with respect to the mounting point of the suction cup, $\text{state}_{\text{scup}}$ the deformation and deformation velocity of the suction cup, $\text{state}_{\text{air}}$ is the state of the fluid (mass flow, volumetric flow, pressure) within the suction cup and in a suitable volume surrounding the suction cup lip and object surface initially in contact with the suction cup lip. Outside of this volume, the fluid is considered to be at rest. The dependency of the total force $f_{\text{scup+air}\to\text{obj}}$ on the object mass m in (4), can be understood by rewriting (3) as

$$m\ddot{h} = -mg + \frac{m}{m_{\text{tot}}}\left(f_{\text{stiff-damp}} + f_{\text{air}\to\text{scup}} + f_{\text{air}\to\text{obj}}\right),$$

leading to

$$f_{\text{scup+air}\to\text{obj}} = \frac{m}{m + m_{\text{sc}}}\left(f_{\text{stiff-damp}} + f_{\text{air}\to\text{scup}} + f_{\text{air}\to\text{obj}}\right)$$

during the first phase of the release. The task at hand is to learn (4) from experimental data. From a practical perspective, only an approximation of the suction cup state (its elongation and its time derivative) and the object state (position with respect to the suction cup mounting point and/or suction cup lip) can be considered to be known. Another straightforward quantity to measure is the instant of time at which the release command is issued to the gripper. The internal state of the air $\text{state}_{\text{air}}$ is, hard, if not impossible to estimate in real-time. For these reasons, we make the following assumption and we will later show in the experimental results that such an assumption has been empirically verified.

Fundamental assumption. *The state of the fluid* state_{air} *and suction cup state*[1] state_{scup} *appearing in* (4) *are, during release, explicit functions of the object state* state_{obj}*, and time* t*, where* t *denotes the time elapsed from the moment the object release command is issued.*

[1]Side note. In lab conditions the suction cup lip position with respect to the suction cup mounting point (and thus $\text{state}_{\text{scup}}$) can be retrieved via the motion capture system, and could thus be used as input for (5). In industrial settings, however, assuming to measure $\text{state}_{\text{scup}}$ would require the modification of the suction cup by including additional sensors, which are currently not available. Using the suction lip state as input is also not desired in terms of robustness, system complexity, and cost perspectives.

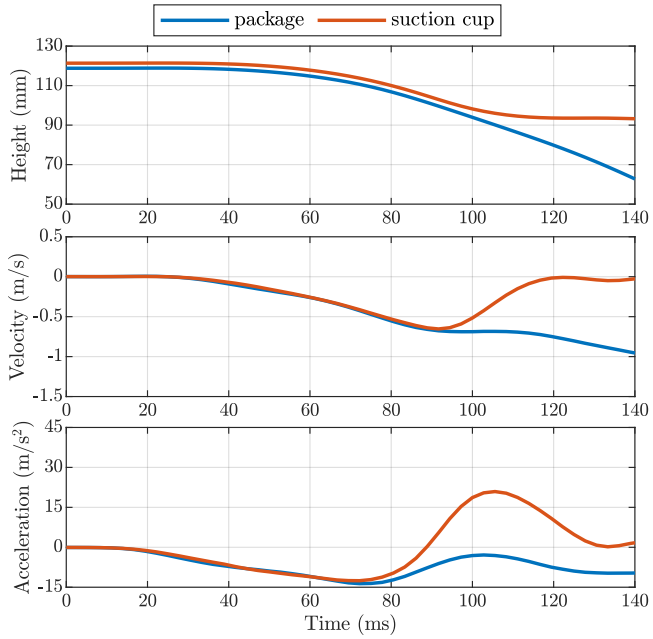

Fig. 4: Typical position, velocity, and acceleration profiles during release. The figure shows both the suction cup lip as well as the package height with respect to the ground. After detachment, the suction cup lip stabilizes to a constant height while the object continues to fall freely.

Given this assumption, (4) can be simplified into

$$f_{\text{scup+air}\to\text{obj}} = f_{\text{scup+air}\to\text{obj}}(\text{state}_{\text{obj}}(t), m, t). \tag{5}$$

The 1D dynamics (1) can therefore be written as

$$m\ddot{h} = -mg + f_{\text{scup+air}\to\text{obj}}(z, \dot{z}, m, t) \tag{6}$$

where z denotes the relative position of the object with respect to the mounting point of the suction cup, as shown in Figure 3b. Defining the height of the suction cup mounting point as a, we can rewrite (6) as (note that $h = a - z$)

$$-m\ddot{z} = -mg + f_{\text{scup+air}\to\text{obj}}(z, \dot{z}, m, t) - m\ddot{a}. \tag{7}$$

Note how $m\ddot{a}$ appearing on the right-hand side of (7) is the apparent force when writing the dynamics in the reference frame of the mounting point, which is non-inertial if $\ddot{a} \neq 0$. Using (7), an estimate of $f_{\text{scup+air}\to\text{obj}}$ is obtained from motion capture data, knowing the object mass. This force estimate is then paired with the relative position z and velocity $\dot{z}$ of the object, the time elapsed since the triggering of the release command t, and mass m. In the following section, we show that a supervised learning approach can be used to predict $f_{\text{scup+air}\to\text{obj}}$ as function of $(z, \dot{z}, m, t)$, allowing for accurate position and velocity prediction.

IV. Empirical validation of the fundamental assumption, model learning, and validation

Vertical release experiments are performed where the experimental object is loaded with different weights. Specifically, release experiments with $m \in \{160, 306, 452, 642, 714, 784, 974, 1181, 1581, 2187\}$ grams are recorded. For each value of m, 11 experiments are executed[2].

[2]All recorded data is made publicly available through the Impact Aware Robotics database, see `https://impact-aware-robotics-database.tue.nl/`.

Typical position, velocity, and acceleration profiles of both the test object and the suction cup lip for a single experiment are shown in Figure 4. Release experiment data is collected over a common time interval $[0, T]$, where T is selected long enough to ensure the object is in free fall towards the end of the interval. A noncausal Savitzky-Golay filter [15], [16] is used to filter the noisy position signal from the motion capture system and estimate the velocity and acceleration after the experiments. In the left plot of Figure 5, we provide the *average* object height for all repeated experiments with the same mass. The figure also provides average velocity and acceleration estimates. For all experiments, at the moment of release ($t = 0$), the object and gripper are at equilibrium, hence ($\dot{z}(0) = \dot{a}(0) = 0$). Different weights lead to quite different acceleration, velocity, and position profiles. Furthermore, objects experience an oscillatory acceleration until the object physically detaches from the suction cup (cf. also Figure 1). Acceleration can then even change sign (the object is being pulled, instead of being pushed by the suction gripper) likely because a still persisting under pressure within the suction cup will force surrounding air to get suddenly inside the suction cup, generating a pulling force on the object. This acceleration inversion lasts for about 20 to 40 ms, after which the object experiences a vanishing force interaction with the suction gripper, and its motion is dominated by gravity. All objects tend to free fall after about 100 ms from the release command, with a constant acceleration, empirically confirming the assumption that aerodynamic drag is negligible for these experiments. The right plot of Figure 5 displays the *average* height a, velocity $\dot{a}$, and acceleration $\ddot{a}$ of the suction cup mounting point for different values of m. The plots show an apperent acceleration of the mounting point during release as result of the dynamic reaction forces at the level of the suction cup. At rest, the suction cup elongation z is a function of mass, as shown in Figure 6. The plot shows the 11 measurements, the average values, and a $\pm 3\sigma$ band. As a general trend, the heavier the attached object, the larger the suction cup elongation becomes.

Learning the force model. The availability of the signals z, $\dot{z}$, $\ddot{z}$, and $\ddot{a}$, allow to estimate $f_{\text{scup+air}\to\text{obj}}$ appearing in (7) for each instant of time and setting up a supervised learning problem, with z, $\dot{z}$, m, and t as input and $f_{\text{scup+air}\to\text{obj}}$ as expected output. Assuming, without loss of generality, that $m\ddot{a}(t)$ is negligible when compared to gravity and suction-cup induced forces, the solution to (7) can be abstractly written as

$$(z(t), \dot{z}(t)) = \phi(t, t_0, z_0, \dot{z}_0; m) \tag{8}$$

with ϕ denoting the flow map of the ODE and where $z_0 := z(t_0)$ and $\dot{z}_0 := \dot{z}(t_0)$. We can further assume that $t_0 = 0$, as we are interested in simulating the system from the moment of release, when the ejector valve is closed and simultaneously air is injected creating a blow-off. From assumption (5) and the *continuity of the solutions* of (7) with

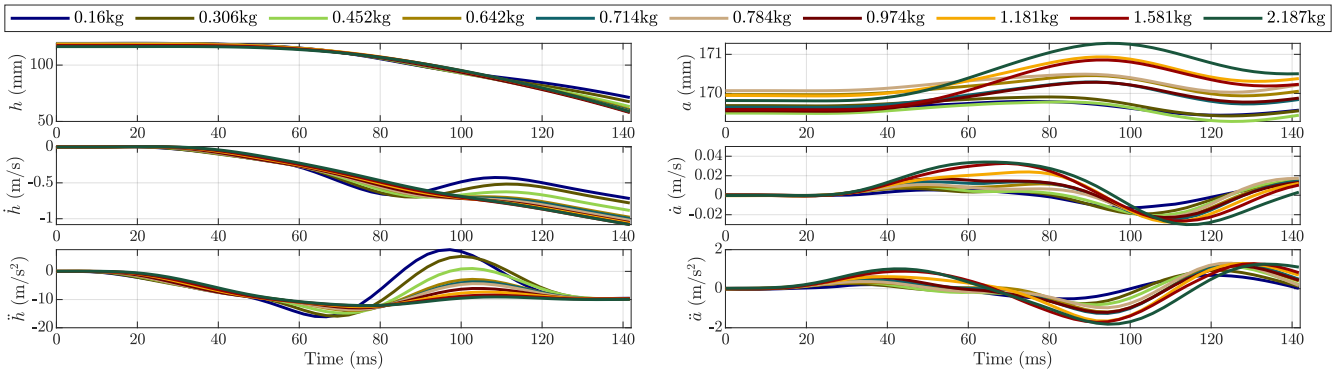

Fig. 5: Position h, velocity $\dot{h}$, and acceleration $\ddot{h}$ of the object (left) and position a, velocity $\dot{a}$, and acceleration $\ddot{a}$ of the mounting point (right).

respect to variations of initial conditions and parameters, one expects that each trajectory $(z(t), \dot{z}(t), m, t) \in \mathbb{R}^4$, $t \in [0, T]$ corresponding to a different initial condition and parameter value $(z_0, \dot{z}_0, m_0)$. would remain separated from the others in the 4-dimensional space.

Visually verifying the lack of self intersection in a 4-dimensional space is not possible, but we have discovered that such a lack of self intersection is actually visible in a 3-dimensional space, provided a suitable mapping is used. In particular, the mapping $\mathbb{R}^4 \ni (z, \dot{z}, t, m) \mapsto (mz, m\dot{z}, t) \in \mathbb{R}^3$ is such a mapping as can be seen in Figure 7a. A priori, there is no reason to expect that the trajectories in the 4-dimensional space should not intersect when looking at a submersion into a 3-dimensional space. However, a lack of intersection in the submersed space actually *implies* lack of intersection in the original four-dimensional space, due to the invertibility of the continuous mapping when restricted to its image. The lack of intersections in the $(mz, m\dot{z}, t)$ space also suggests that it is possible to then learn the force model f using the reduced coordinates $(mz, m\dot{z}, t)$ in place of $(z, \dot{z}, m, t)$ and thus assume that

$$f_{\text{scup+air}\to\text{obj}} = f_{\text{scup+air}\to\text{obj}}(mz, m\dot{z}, t). \tag{9}$$

In the following, we show that by employing this reduced set of coordinates, we can indeed learn a force model that reproduces accurately the measured object position, velocities, and accelerations even for a test mass that was not included in the training data. The training-validation split is such that data pertaining to one specific object mass is used to validate, while the rest is used to train the force model. Having obtained a force model, its efficacy is evaluated by using it in simulation for the validation mass and comparing the predicted trajectory with the measured one. This is then done for all masses. This is referred to a cross-validation.

It is worthwhile to note that learning the force model using other reduced parameterizations might lead to poor results. For example, the coordinates $(z, \dot{z}, t) \in \mathbb{R}^3$, that were initially considered, do not produce valuable results. The trajectories in this 3-dimensional space, as illustrated in Figure 7b, actually twist and intersect in a region of the space, preventing to learn a single-valued force function using these coordinates as inputs. An additional problem is that at time $t = 0$, the trajectories of the various experiments

TABLE I: Table with LWPR algorithm settings.

Parameter	Value	Parameter	Value
kernel	Gaussian	init_D	560
norm_in	[0.257, 2.585, 0.139]	diag_only	0
init_alpha	250	w_gen	0.2
meta	1		

for different m actually overlap, as can also be observed from Figure 6. What is problematic in this set of coordinates is, in particular, that there is no dependence on the object mass, while such a dependence is to be expected as we detailed in Section III.

To learn the force model, we have employed the *Locally Weighted Projection Regression* (LWPR) incremental learning approach [17] and employed the freely available implementation [18]. LWPR is a machine learning approach for nonlinear function approximation that learns incrementally in (potentially) high-dimensional spaces. This method was used because it is a well established method, and because in the future we will use it on a highly dimensional input space corresponding to the full 6D dynamics. Consider Figure 8. The figure shows that by employing LWPR to learn the function $f_{\text{scup+air}\to\text{obj}}(mz, m\dot{z}, t)$ from experimental data, we obtain quite accurate predictions of the motion of the object during release, for an experiment that was *not* included in the training set. More specifically, for each value of m, a force model is learned using the experiments with a different mass and then a simulation is performed by integrating (7) using m, the average acceleration $\ddot{a}(t)$, and the average initial condition $z(0)$ and $\dot{z}(0)$ from the experiments related to that value of m. Not surprising, the predictions are poorer for the edge cases ($m = 2187$g, but especially for $m = 160$g) as they correspond to extrapolation rather than interpolation. Excluding these edge cases, the *maximum absolute error* of the predicted trajectory from the average motion obtained from the experiments is of 2.14mm for the position, 0.09m/s for the velocity, and 2.65m/s^2 for the acceleration, respectively. The *root-mean-square error*, again excluding the edge cases, is 0.75mm, 0.023m/s, and 0.381m/s^2, respectively. For completeness, the LWPR algorithm settings that were used for training are given in Table I[3].

[3]The code that is used to obtain the results, is made publicly available through `https://gitlab.tue.nl/robotics-lab-public/learning-1d-suction-cup-dynamics`

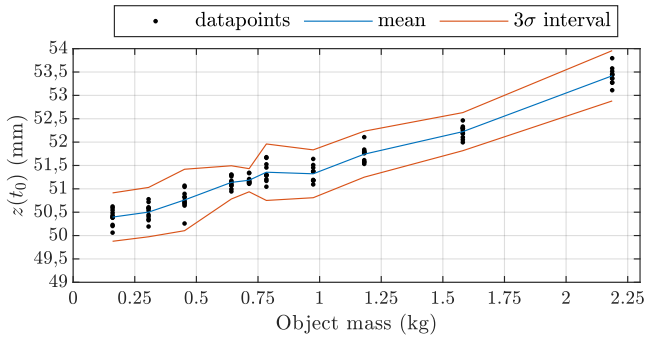

Fig. 6: Suction cup rest length versus object weight. The blue line denotes the average and the red curve the $\pm 3\sigma$ band.

V. Conclusion and Future Work

In this paper, we have considered the vertical motion of objects of known mass released from an active vacuum suction gripper. The motion of the objects and the suction cup mounting point are recorded via a motion capture system. A supervised learning approach is proposed that shows remarkable prediction capabilities when evaluated on a test set, despite not having any direct information about the suction cup state. Learning the force model can be cast as a function approximation problem in a three-dimensional space (mass-scaled relative position and velocity and elapsed time) instead of a four-dimensional space (relative position, relative velocity, mass, and elapsed time). This allows for visual inspection of the measurement data for assessing, e.g., its regularity. However, selecting a suitable 3-dimensional embedding is crucial, as the embedding using relative position, relative velocity, and elapsed time, as initially chosen, leads to poor predictions. The generalization and validation of the approach for planar and full spatial motions are left for future work. The extension to learning a multi-dimensional force-torque model, likely requires the use of the relative position, orientation, linear and angular velocity, and the object's inertia tensor as input. This problem setting is significantly more complex. However, achieving an accurate prediction of the 1D force shows that the assumption of (5) is valid, giving good hope that the same approach can be used in the 6D case. Obtaining an accurate prediction of the 6D object motion during release from a suction gripper is useful for motion planning for robotic tossing, either on surfaces such as conveyor belts or into boxes and totes. Another direction for future research is the investigation of force models for objects with different surface sealing. We expect that, via a pressure sensor, sealing conditions can be identified before release, acting as a prior in selecting the correct learned model. In this work, considering the generalization to the 6D case, the LWPR method is selected because it showed excellent performance in learning the flying dynamics of rigid-bodies from motion capture data [19]. Also in the context of this paper its performance is excellent. However, the hyperparameters should be systematically tuned over a validation set. Likewise, a comparison with other learning methods should be made.

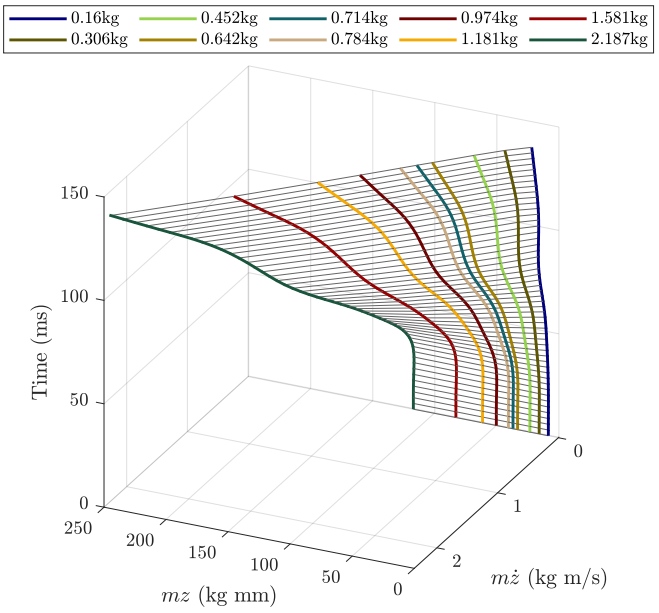

(a)

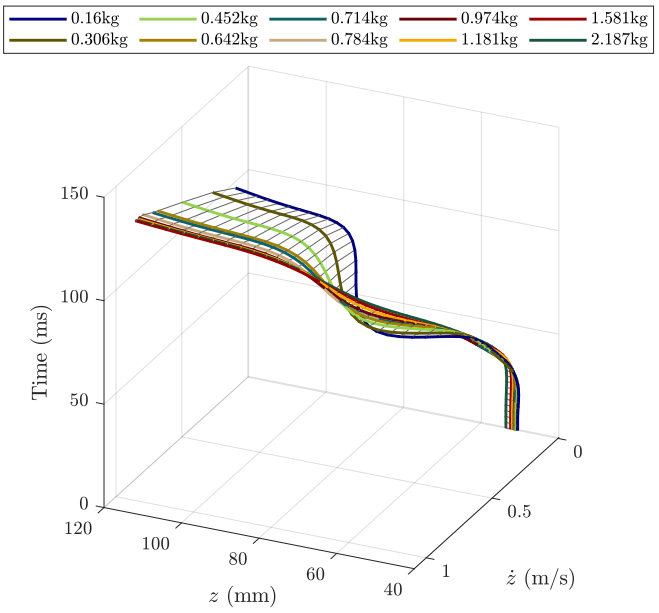

(b)

Fig. 7: The average measured trajectories visualized in (a) the $(mz, m\dot{z}, t)$ space and (b) the $(z, \dot{z}, t)$ space. Curves in using the second parametrization twist and intersect in the middle of the time interval, hindering the learning of a force model using these coordinates.

References

[1] "Smart Item Robotics," https://www.vanderlande.com/systems/picking/smart-item-robotics/, Vanderlande, 2022, [Online; accessed 29-Jun-2022].

[2] R. Shome, W. N. Tang, C. Song, C. Mitash, H. Kourtev, J. Yu, A. Boularias, and K. E. Bekris, "Towards robust product packing with a minimalistic end-effector," in *IEEE International Conference on Robotics and Automation (ICRA)*, 2019, pp. 9007–9013.

[3] J. Mahler, M. Matl, X. Liu, A. Li, D. Gealy, and K. Goldberg, "Dex-Net 3.0: Computing Robust Vacuum Suction Grasp Targets in Point Clouds Using a New Analytic Model and Deep Learning," in *IEEE*

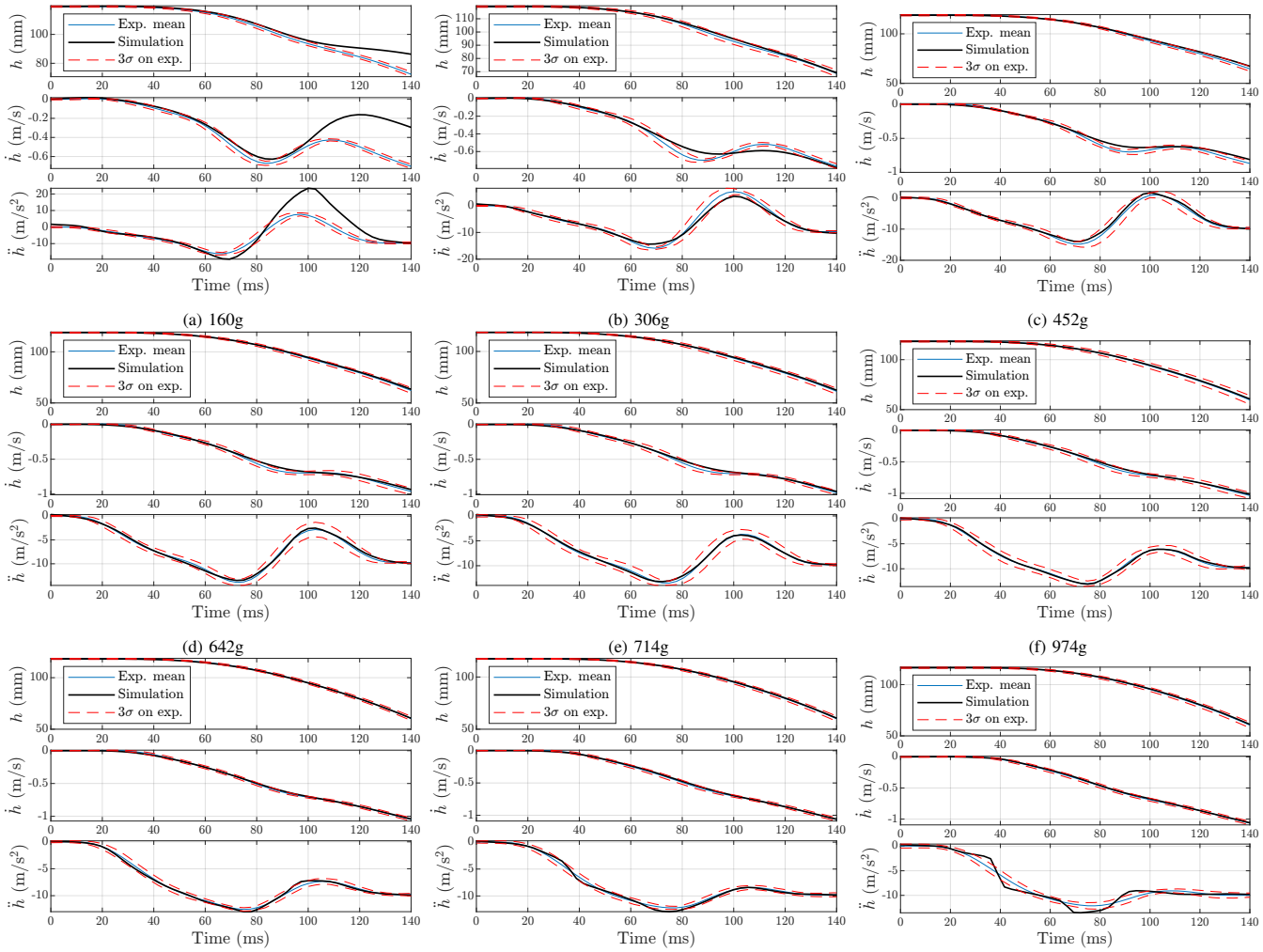

(a) 160g (b) 306g (c) 452g

(d) 642g (e) 714g (f) 974g

(g) 1181g (h) 1581g (i) 2187g

Fig. 8: Predicted vs measured object height, velocity, and acceleration for a selection of object weights. Average measured object trajectories are plotted in blue, with 3σ intervals shown in red. The model prediction is shown in black. Edge cases (a) and (i) are not expected to be accurate, as they correspond to extrapolation of the experimental data.

International Conference on Robotics and Automation (ICRA), 2018, pp. 5620–5627.

[4] X. Cheng, Y. Hou, and M. T. Mason, "Manipulation with Suction Cups using External Contacts," in *International Symposium on Robotics Research (ISRR)*, 2019, pp. 1–16.

[5] C. Correa, J. Mahler, M. Danielczuk, and K. Goldberg, "Robust toppling for vacuum suction grasping," in *IEEE International Conference on Automation Science and Engineering (CASE)*, 2019, pp. 1421–1428.

[6] "Zen robotics fast picker," https://zenrobotics.com/fast-picker, Zen Robotics, 2022, [Online; accessed 29-Jun-2022].

[7] "Robotics plastic recycling video," https://www.amprobotics.com/plastic, AMP Robotics, 2022, [Online; accessed 29-Jun-2022].

[8] "Max AI AQC-C cobot," https://www.max-ai.com/video-max-ai-autonomous-qc/, MAX-AI, 2022, [Online; accessed 29-Jun-2022].

[9] F. Raptopoulos, M. Koskinopoulou, and M. Maniadakis, "Robotic Pick-and-Toss Facilitates Urban Waste Sorting," in *IEEE International Conference on Automation Science and Engineering (CASE)*, 2020, pp. 1149–1154.

[10] A. Betnardin, C. Duriez, and M. Marchal, "An Interactive Physically-based Model for Active Suction Phenomenon Simulation," in *IEEE/RSJ International Conference on Intelligent Robots and Systems (IROS)*, 2019, pp. 1466–1471.

[11] A. Tiwari and B. N. J. Persson, "Physics of suction cups," *Soft Matter*, vol. 15, pp. 9482–9499, 2019.

[12] H. Pham and Q. C. Pham, "Critically fast pick-and-place with suction cups," in *IEEE International Conference on Robotics and Automation (ICRA)*, 2019, pp. 3045–3051.

[13] N. Dehio and A. Kheddar, "Robot-Safe Impacts with Soft Contacts Based on Learned Deformations," in *IEEE International Conference on Robotics and Automation (ICRA)*, 2021, pp. 1357–1363.

[14] F. Gabriel, M. Fahning, J. Meiners, F. Dietrich, and K. Dröder, "Modeling of vacuum grippers for the design of energy efficient vacuum-based handling processes," *Production Engineering*, vol. 14, no. 5-6, pp. 545–554, 2020.

[15] A. Savitzky and M. J. E. Golay, "Smoothing and Differentiation of Data by Simplified Least Squares Procedures," *Analytical Chemistry*, vol. 36, no. 8, p. 1627–39, 1964.

[16] R. W. Schafer, "What Is a Savitzky-Golay Filter?" *IEEE Signal Processing Magazine*, vol. 28, no. 4, pp. 111–117, 2011.

[17] S. Vijayakumar, A. D'Souza, and S. Schaal, "Incremental Online Learning in High Dimensions," *Neural computation*, vol. 17, pp. 2602–34, Jan. 2006.

[18] "Locally Weighted Projection Regression," https://web.inf.ed.ac.uk/slmc/research/software/lwpr, University of Edinburgh, 2019, [Online; accessed 29-Jun-2022].

[19] S. Kim and A. Billard, "Estimating the non-linear dynamics of free-flying objects," *Robotics and Autonomous Systems*, vol. 60, p. 1108–1122, Sept. 2012.